Twisted Contact Structures in Turbulent Flows

Horia DUMITRESCU[1], Vladimir CARDOS*[,1], Radu BOGATEANU[2]

*Corresponding author
*[,1]"Gheorghe Mihoc – Caius Iacob" Institute of Mathematical Statistics and Applied Mathematics of the Romanian Academy,
Calea 13 Septembrie no. 13, 050711 Bucharest, Romania,
dumitrescu.horia@yahoo.com, v_cardos@yahoo.ca*
[2]INCAS – National Institute for Aerospace Research "Elie Carafoli",
B-dul Iuliu Maniu 220, Bucharest, 061126, Romania,
bogateanu.radu@incas.ro, unquradu@gmail.com

DOI: 10.13111/2066-8201.2019.11.1.7

Received: 22 January 2019/ Accepted: 19 February 2019/ Published: March 2019
Copyright © 2019. Published by INCAS. This is an "open access" article under the CC BY-NC-ND license (http://creativecommons.org/licenses/by-nc-nd/4.0/)

International Conference of Aerospace Sciences "AEROSPATIAL 2018"
25 - 26 October 2018, Bucharest, Romania, (held at INCAS, B-dul Iuliu Maniu 220, sector 6)
Section 1 – Aerodynamics

Abstract: *The "hairpin" vortical structure initiated from a conceptual model of Theodorsen refers to a Ω-shaped vortex with two streamwise-oriented legs connected via a raised spanwise-oriented arch. Both computational and experimental studies in flow visualization revealed considerable disagreement as to the underlying hairpin vortex generation mechanism as well as its interpretation. The goal of this paper is to give a deeper insight of this key issue closely related to the turbulence as a dynamic stochastic phenomenon involving the origin and its generation mechanism. The topological concept of twisted contact structures associated with vorticity concentrations in wall-bounded flows strongly contorted at the starting-time is used to explain the genuine structured turbulence of Lagrangian nature at sufficiently large Reynolds numbers. The dynamical stochastic models of starting impact permit to identify two intrinsic scales for describing the starting impact-wall twist relationship generating a local turbulence mechanism. The inertia scale (rate of inertia, e) and circulation scale (azimuthal wave length, π) are measures for impact and twist, respectively, the turbulence lying in their dynamics like a torsion pendulum mechanism. The intrinsic scales of molecular nature have an interesting correspondence in macro-flow field through two relativistic well-known parameters: Mach number and Reynolds number playing the role of some reduced amplitudes and frequencies of the compressibility waves generated by the starting impact/shock. The maximum amplitude* $M_\infty = 2/3$ *defines a critical Reynolds number* $\mathrm{Re}_{scr} \equiv 1/2\rho_0 a_0^2 = 2/3\cdot 10^5\, N/m^2$ *(a_0 –sound velocity of air at rest), numerically equal to the maximum impact pressure where the frictional shearing stress is near annulled, and its inverse value is the equilibrium kinematic viscosity* $\nu_0 = 1.5\cdot 10^{-2}\, m^2/s$ *or the stable minimum circulation at a contact surface. These reference dimensional quantities are used to a more comprehensive definition of the current Reynolds numbers as the ratio of* (V_∞^2/ν_0) *contact to* (V_∞/l) *outer flow frequencies. Then, it is shown that the wave behavior of wall-bounded flows have a universal character (regardless of much diversity of flow cases) where the wall torsion pressure and the frictional wave drag are more realistic models than Lighthill's boundary vorticity flux (BVF) mechanism and semi-empirical Prandtl's wall law.*

Key Words: *Laminar-turbulent transition, shear turbulence, coherent hydrodynamic structures, vortex dynamics*

1. INTRODUCTION

The fluid flows without definite shape involve a motion guided by solid surfaces/boundaries contorting flow field, i.e. the streamline pattern, in their vicinity. The far motion field of fluid is naturally a plane field governed by Euler equation for an ideal/perfect, i.e. incompressible and inviscid, fluid. However, the concept of a perfect fluid fails completely to account for the drag of bodies in a fluid environment (d'Alembert's paradox [1]). This unacceptable result of the theory of a perfect fluid is a consequence of the fact that the wall-bounded flows of a real fluid transmit shearing friction (i.e. damped perturbations) as well as rolling friction (i.e. self-sustained perturbations) stresses as the Reynolds number increases. This friction forces in a real fluid are connected with the noteworthy properties of shear (linear/Newtonian effect) and torsion/twist (nonlinear effect) of the viscosity, exhibited during the onset of motion at fluid-solid contact surfaces. The existence of shearing friction stresses along with the condition of no slip near solid walls have constituted the essence of the Prandtl's boundary-layer theory [2] that could solve only the d'Alembert's paradox, the turbulence problem remaining as a long-lasting and continuing paradigmatic crisis in the basic research of fluid dynamics. Herein a number of authors consider that turbulence is a manifestation of breakdown of the Navier-Stokes equations (NSE) [3], [4], [5], [6], though they commonly believe that the NSE-solutions correspond (at best) to real fluid flows.

Our recent papers [7], [8] have shown that the existence of rolling friction stresses and a slip condition ("no slide-slip" condition) at solid walls constitute the essential differences between the Newtonian viscous fluid, damping the small perturbations at fluid-solid contact surfaces, and a visco-elastic/thixotropic fluid, adjusting itself with the flow state. To a greater or lesser extent, most fluid materials exhibit elastic share behavior which can support torsion/twist stresses of concentrated vorticity created at a fluid-solid contact surface at start up. The torsion stress state is exhibited as compressing vorticity waves generated by a fast non-inertial motion of Lagrangian nature, termed "structured turbulent/contact" flow in contrast to the conventional structureless turbulent flow containing random residual vorticity transported by the Eulerian flow. The fast contact motions are the internal/intrinsic intermittent motions associated with spotty temporal and spatial patterns of the small scale vortical structures, in contrast to the observable external intermittent motions associated with the random movement of residual vorticity superimposed on an Eulerian basic flow. The lack of shear elasticity in fluid leads to the impossibility of fast fluid-solid contact motions or the formation of compressing vorticity waves, which are the key to origin and mechanisms of turbulence.

Though most of the practical aspects of turbulence were solved by experiments, theoretically persists the lack of success of the NSE concerning the existence of a gap between the scales of molecular motions and the smallest relevant scales in turbulent flows, i.e. the fast contact motions inducing exponential growth of a vortical field concomitantly with vorticity dispersion.

The current paper shows how this impediment of paradigmatic nature can be overcame by using the concept of twisted contact structures, in particular the vorticity concentrations in wall-bounded layers strongly contorted. At the same time, the concentrated boundary vorticity explains the Ω-shaped/"hairpin" vortical structures and their complex dynamic of Lagrangian nature.

2. THE TOPOLOGICAL CONCEPT OF TWISTED CONTACT STRUCTURES

The contact topology is connected to the notion of contact transformation introduced by S. Lie [9] as a geometric tool to study systems of differential equations. The subject has manifold connections with other fields of pure mathematics, and a significant place in applied areas such as mechanics and thermodynamics where the turbulence problem is based on a rather a complicated mathematical theory on contact geometry.

Contact transformations. Following Lie, a contact element of $\mathbf{R}^2$ or line element is defined to be a point $(x,y)\in\mathbf{R}^2$ and a line passing through this point. As long as the slope p of this line is finite, the equation for this line may be written in the form

$$dy-pdx=0\,, \tag{1}$$

and the space of such contact elements can be identified with $\mathbf{R}^3$ with coordinates (x, y, p). Now a solution $y=y(x)$ of a differential equation $F(x,y,y')=0$ corresponds to an integral curve $X\to(y,y(x),y'(x))$ of the plane field on $\mathbf{R}^3$ given by (1). Therefore, a transformation

$(x,y,p)\to(x_1,y_1,p_1)$ is called a contact transformation if

$$dy_1-p_1dx_1=\rho(dy-pdx)$$

for some nowhere zero function $\rho:\mathbf{R}^3\to\mathbf{R}$. The transformations of this sort show that carry systems of integral curves of a differential equation $F(x,y,y')=0$ to systems of integral curves of the transformed equation $F_1(x_1,y_1,y_1')=0$.

In planar geometry there are two typical contact transformations: 1) the mapping of a curve γ in $\mathbf{R}^2$ to a parallel curve γ_1 at distance $k\in R^+\,(\gamma\to\gamma_1)$ of the form

$$\begin{aligned}(x_1-x)+(y_1-y)\,p&=0\\ p_1&=p\end{aligned}\,, \tag{2}$$

or

$$\begin{aligned}x_1&=x\pm\frac{kp}{\left(1+p^2\right)^{1/2}}\\ y_1&=y\pm\frac{p}{\left(1+p^2\right)^{1/2}}\end{aligned}\,, \tag{2'}$$

is a contact transformation called “dilatation”; 2) any given differentiable curve $\gamma(t)=(x(t),y(t))$ can be associated with another curve $\gamma_1(t)=(x_1(t),y_1(t))$, defined by the condition that $(x_1(t),y_1(t))$ be the pole of the tangent to $\gamma(t)$ at $(x(t),y(t))$, and this new curve $\gamma_1(t)$ called the polar transformation of $\gamma(t)$ is given as

$$\left(x,y,p=\frac{dy}{dx}=\frac{\dot{x}}{\dot{y}}\right)\to\left(x_1=\frac{-p}{y-px},y_1=\frac{1}{y-px},p_1=-\frac{x}{y}\right), \tag{3}$$

with $dy_1 - p_1 dx_1 = -\dfrac{1}{y(y-px)}(dy - pdx)$.

The polar transformation of $\gamma_1(t)$ recovers $\gamma(t)$. These particular contact transformations are well illustrated by Apollonius circles (Fig. 1) showing geodesic like curves (dilatation transformation) and Legendrien like curves (polar transformation).

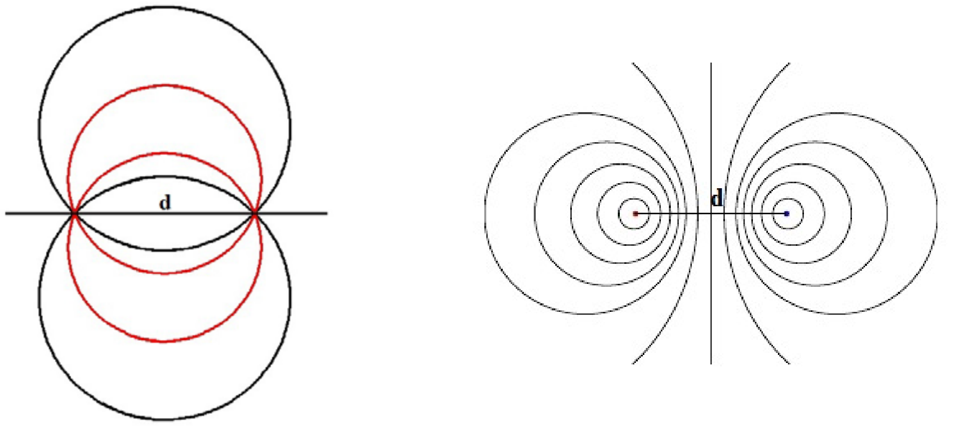

a) b)

Figure 1 – Contact transformations illustrated by Apollonius circles: a) dilatation (geodesic-like curves); b) polar (Legendre-like curves)

Topological definition. There is also a modern mathematical description of a contact structure as a 3- differentiable manifold *M* that is a completely nonintegrable tangent plane field ξ [10]. The complete nonintegrability of ξ can be expressed by the inequality $\alpha\Lambda dx \neq 0$ for a 1-form α which locally defines the plane field $\xi = \ker\alpha$, i.e. $\xi = \{\alpha = 0\}$. The sign of the form $\alpha\Lambda d\alpha$ is independent of the sign of α and, therefore, a contact structure ξ defines an orientation of the manifold *M*. For a 2-surface $F \subset M$ in a contact 3-manifold (M,ξ), generically *F* is tangent to ξ in a finite set $\Sigma = \{p_1, p_2, ..., p_k\} \subset F$. Outside Σ the contact structure ξ intersects $T(F)$ along a line field *K* which integrates to a 1-dimensional foliation on *F* with singularities at points of Σ. This singular foliation on *F* is called the characteristic foliation of *F* denoted by F_u. The foliation F_ξ.is always locally orientable and the line field *K* at its singularities is well defined by an index ± 1: a singular point $p \in S$ elliptic if its index is +1 and hyperbolic if it is -1. The foliation F_u has a focus type singularity in an elliptic ξ point, and a saddle type singularity in a hyperbolic one (Fig. 2), that topologically are indistinguishable. The characteristic foliation F_ξ defines the germ of a contact structure along *F*.

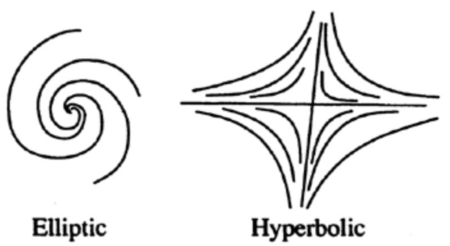

Figure 2 – Singularity types a) elliptic (focus); b) hyperbolic (saddle)

Twisted disc structure. On the other hand, the contact geometry more or less is present for any solid/fluid motion where its configurational space $\mathbf{R}^3$ with coordinates $u=(x,y)$ on $\mathbf{R}^2$ describes a hyperplane/tangent plane field $T_u\mathbf{R}^2$ by the local noslide-slip condition

$$\sin(\theta)\delta x-\cos(\theta)\delta y=0$$

and S_1 is identified with $\mathbf{R}/2\pi\mathbf{Z}$ as an element θ of $\mathbf{R}/\pi\mathbf{Z}=\mathbf{R}P^1$ (a projective space). The above condition written in a differential form as

$$\xi_u=\ker\left(\sin(\theta)dx-\cos(\theta)dy\right), \tag{4}$$

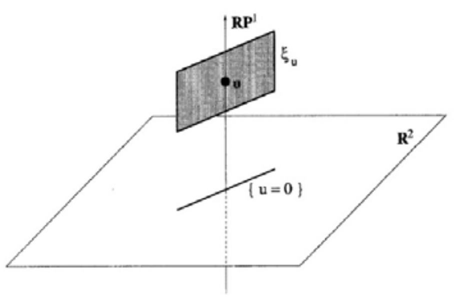

a)

b)

Figure 3 – Natural contact structure a) the space of contact elements ($u=0$ - fixed point); b) plans ($\mathbf{R}^2$) rotating around vertical lines ($\mathbf{R}P^1$)

describes a natural contact structure on the space of contact elements $\mathbf{R}^2\times\mathbf{R}P^1$ (Fig. 3). The moving wheel/disk describes a Legendre curve in the space of contact element of the plane with its natural contact structure. The change from this simple/trivial topology to the contact structures on closed 3 manifolds is defined by Lutz twist [11] as any curve that winds at least once around the origin (Fig. 4a).

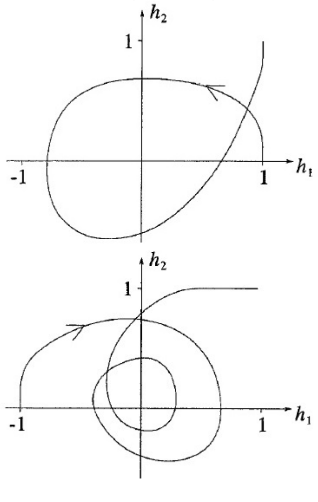

a)

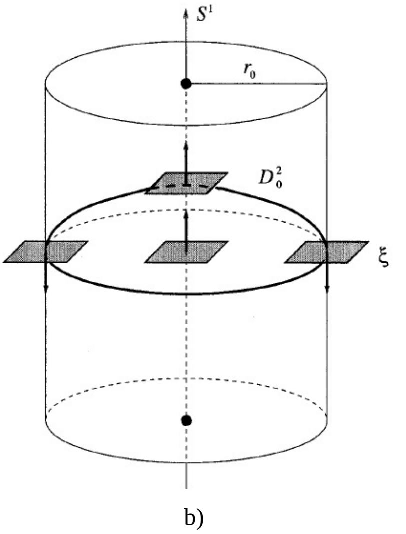

b)

Figure 4 – Twisted contact structure: a) Lutz twists; b) twisted disc model (($u=0$ - free point)

For a topologically non-trivial Lutz twist, the cut $S^1 \times D^2 \subset S^1 \times \mathbf{R}^2$ and gluing back $D^2 \times S^1$, are identified by

$$\partial\left(S^1 \times D^2\right) = S^1 \times S^1 = \partial\left(D^2 \times S^1\right),$$

where $S^1 \times \mathbf{R}^2$ is a contact form $\alpha = d\theta + r^2 d\varphi$ with S_1 – azimuthally coordinate, θ and (r,φ) - polar coordinates on $\mathbf{R}^2$. One can find a disk D_0^2 embedded in $S^1 \times D^2$ such that ∂D_0^2 is tangent to $\xi = \ker\alpha$, but D_0^2 is transverse to ξ along ∂D_0^2 (Fig. 4b). In this figure, r_0 denotes the smallest positive radius where the contact plane has made a rotation by π around the radial axis. Such a contact structure is known as an over twisted disk structure on orientable 3 – manifolds.

The twisted disc structure is the basic topological model for the understanding of turbulence processes, where π is a sort of azimuthally wave number for flows with the rapidly developing field of contact topology, of their evolution is given by the Reynolds number (more exactly $\log \mathrm{Re}_l$): $\log \mathrm{Re}_l \geq \pi$ - twist (laminar flow), $\log \mathrm{Re}_l \geq 2\pi$ - twist (turbulent flow), and $\log \mathrm{Re}_l = 3\pi$ is the end/“death” of the turbulence process. The twisted contact structure is a more realistic model able to characterize “turbulence” in terms of the dynamics of twisted contact structure.

3. FLUID-DYNAMIC COHERENT/CONTACT STRUCTURES

The fluid-dynamic problems associated with various aspects of the evolution of vortical movements are exceptionally important both in terms of practical applications and the study of such flows with rapidly developing wall vortical structures. The contact topology can establish a close relationship between the fields of fluid-dynamics on Riemannian manifolds and their contact structure setting in during the starting impact.

The study of a viscous fluid-dynamic system based on the NSE for smooth Gaussian starting impact [7] with contact twist less 2π involves only frictional shearing stresses, the mathematical problem becoming an initial (IC) and boundary (BC) condition one which along with the hypotheses of viscous Newtonian fluid and no slip near solid walls removed the d’Alembert’s paradox of Euler equations. The principle of equal action and reaction in the case of contact twist less 2π, i.e. $\mathrm{Re}_l \leq 10^{2\pi}$, is subtly satisfied by means of shearing friction, and the NSE and (IC+BC) problem is a closed one for time-dependent two-dimensional flows for the paradigmatically limited Reynolds number range, that is no solutions for transitional and turbulent flows exist in the framework of the classical NSE theory [6], for any large Reynolds number. For a violent non-Gaussian starting impact, associated with the occurrence of a twist greater than 2π (Lutz twist) of wall-bounded flows, the presence of the complex dynamics of various vortex types (including fast processes of their confluence into successive agglomerations and disintegrations) induces relativistic effects canning identified than in the phase plane as energy states/levels and their orbits. These effects are connected to the formulation of thermodynamics in terms of contact geometry going back to the work of Gibbs [12]. Referring to [7] it is a matter of the molecular thermal energy (or Gibbs free energy) released by the change of fluid microstructure and the creation of the twisted/ concentrated contact vorticity state following a ballistic impact. The dust-vorticity flow is similar to the dusty plasmas [13].

The fact that a contact structure on a three-manifold is a maximally non-integrable tangent plane field ξ (locally defined as $\xi = \ker\alpha$ with a differential 1-form α for $\alpha \Lambda d\alpha \neq 0$ on its whole domain of definition) represents a long fixture in the literature on contact geometry. However, the most of "consumers" of turbulence from those concerned with pure basic issues [4] to people dealing with diverse application believe that NSE are adequate for describing turbulent flows and would expect that NSE possess smooth solutions in a global sense, i.e. for all times and for any large Reynolds numbers. The main goal of this paper is to establish the limits of NSE frame.

The essence of all questions lies in the mass point approximation which depends on the surface molecular tension (skin friction) and the size of the germ of contact structure containing a number of molecules relevant in fluid mass. For the onset of plane motions there are two behaviors illustrated in Fig. 5 (a,b):

a) **continuous contact structure** defined by the material surface $B(\mathbf{x},t)=0$ and the kinematic boundary condition

$$\frac{DB}{Dt} = \frac{\partial B}{\partial t} + \mathbf{u} \cdot \nabla B = 0\,, \tag{5}$$

with stagnant/fixed mass points ($y=0:\mathbf{u}=0,\mathbf{a}=0$, no slip condition, Fig. 5a) for linear viscous/laminar flows;

b) **free point contact structure** called twisted disc and defined by

$$\xi(x,y,p) = \ker(dy - pdx)\,, \tag{5'}$$

and tangent plane field $F_\xi(x) = (x, y(x), p(x))$ with free mass points ($y=0:\mathbf{u}=0,\mathbf{a}\neq 0$, no slide-slip condition, Fig. 5b) for non linear viscous/turbulent flows.

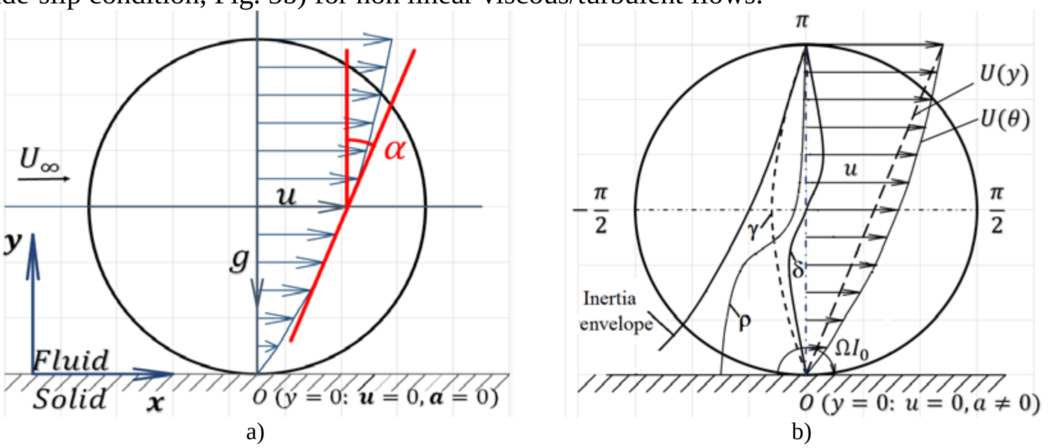

Figure 5 – Material point models: a) surface material structure; b) twisted disc structure with (ρ, γ, δ) wall shear waves (relativistic effect).

In contrast to the continuous contact structure which involves dissipative kinematic effects (without fluid microstructure changes), the twisted contact structure following a ballistic starting impact induces dispersive dynamic effects with fluid-microstructure changes and release of intrinsic energy in the form of vorticity waves.

A starting impact (cause)-turbulence (effect) relationship via wall twisted strain can be easily obtained by means of the twisted disc concept and a hypothesis of thixotropic fluid

[7], [8] adjusting itself continuously with flow state. The thixotropic fluid model has capabilities describing the small scale vortical motions of Lagrangian nature produced by twisted contact structures.

Now, the physical explication of the origin of turbulence phenomenon is rather simple and it resides in the early/latent compressibility effect triggered off at starting when the Mach number exceeds the value of $M_\infty = 1/3$ accepted as the limit for incompressible gaseous (air) flows. The starting compressibility effect becomes active for the Mach number range of $M_\infty = (1/3 - 2/3)$ and these gaseous flows can be called precompressible flows (see par. 4). In the case of liquids, materials with a definite volume, their flows are little different, being affected by the gravitational force, and the dimensionless Froude number ($Fr = V/\sqrt{gd}$). The Froude number is the relativistic parameter (ratio of inertial and gravitational forces) which replaces in this way the Mach number when a liquid flow is considered. It is a measure of potential energy where for $Fr \geq 1/2$ and $\mathrm{Re}_{der} \approx 10^{2\pi}$ the wall-twisted liquids generate themselves small scale-structured turbulence, cinematically of Lagrangian nature and dynamically of molecular thermal nature (with free Gibbs energy). The $\mathrm{Re}_{der} = 1/2 \cdot 10^{2\pi}$ number is the dynamically critical Reynolds number when the twisted contact structure reaches the value of 2π, and its inverse $\nu_0 = 2 \cdot 10^{-2\pi} \approx 10^{-6} m^2/s$ is numerically equal to the kinematic viscosity, i.e. the minimum statically stable circulation at the wall. Soon after reaching this Reynolds number and for $Fr > 1/3$ a wall cavitation-like phenomenon is produced.

In contrast to the intrinsic/internal structured turbulence, there are also large scales – external shear turbulence of inertial nature for $\mathrm{Re}_{scr} \geq 2 \cdot 10^{\pi}$ where the wall frictional shearing stress is statically stable. The regime of non-linear boundary layer instability on the flat plate in a low-turbulence level water channel was investigated (measurement and visualization at $\mathrm{Re}\,(l = 1m) \approx 2 \cdot 10^5$ [14]. However, although the formation process of soliton-like coherent structures (SCSs) has been clearly visualized, for this Reynolds number the onset of concentration and rolling process of vorticity have not been identified, the Reynolds number being lower than its critical value, $\mathrm{Re}_{der} \approx 10^{2\pi}$.

The internal structured turbulence along with itself – sustaining mechanism is a universal process in fluid (gaseous or liquid) motion if the Reynolds number exceeds its dynamically critical value. Though the turbulence is easily observed, its origin has caused a long controversial dispute in the literature on this topic concerning almost every physical and mathematical aspect. This state of matters can be qualified as a long-lasting and continuing paradigmatic crisis seen as a new paradox-paradox of turbulence [15]. The quintessence of the turbulence phenomenon, as origin and mechanism, has been obscured due to its molecular nature in spite of a lot of details were disclosed experimentally with modern-day physical and numerical tools.

4. DYNAMICAL STOCHASTIC MODELS OF STARTING IMPACT

The rest-motion state change is an impact kind called starting impact where a process of momentum and/or energy exchange, with zero-mass flux, between two colliding bodies is produced within a short time of contact. The loading behavior in such process acting with high intensity during a short period of time, is based on a rather complicated theory on contact geometry and statistical mechanics. The starting behavior, vital for the fluency/continuity of motion of any material continuum, is closely related to two intrinsic properties of the physical system possessing opposite tendencies: restoring force (near slide frictionless twisting of molecular nature) and inertia/impact force of gravitational nature. The simplest impact-twist dependence is the near harmonic oscillation called torsion pendulum, modeled by the Duffing equation, with two behavior types depending on the inertia-twist relationship, as regular torsion pendulum (more inertia) and inverted torsion pendulum (more twist) [16].

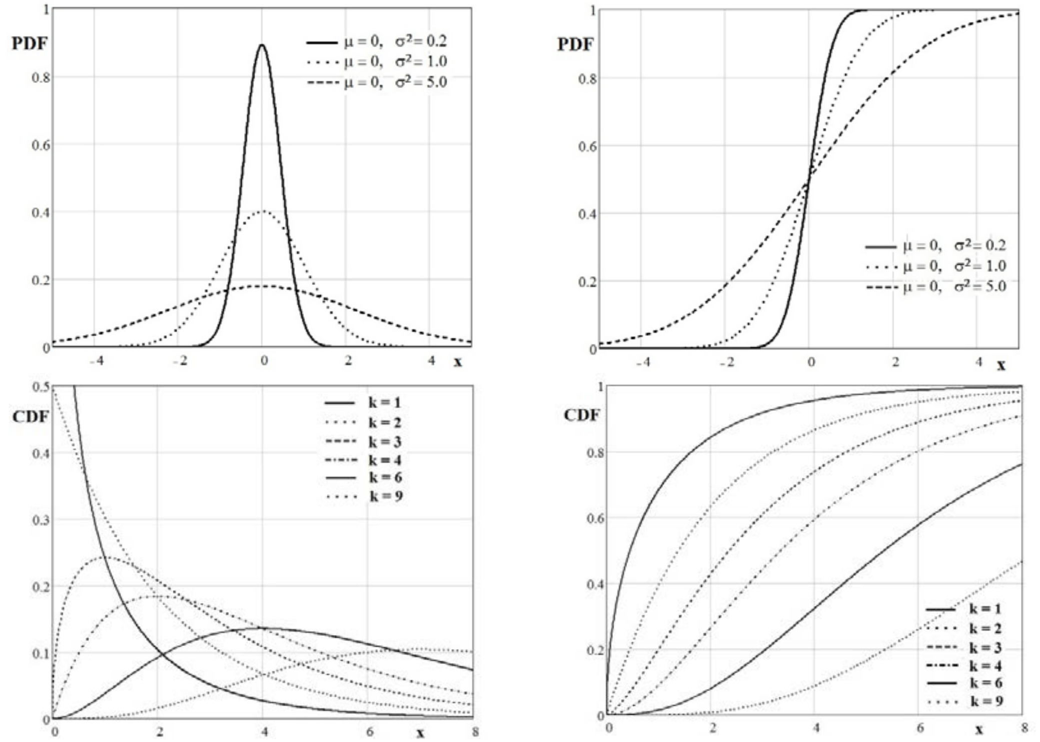

a) b)

Figure 6 – Stochastic models for starting impact: a) normal/Gaussian distribution; b) chi-squared distribution

Generally, an impact/contact problem is connected to the statistical mechanics in Gibbs' phase space. Thus, the starting impact can be either a weak interaction (random impact) with non-microstructure change described by the Gaussian distribution model, or a strong interaction (ballistic impact) with molecular microstructure change, modeled by a non-Gaussian (chi-squared distribution) model (Fig. 6 a, b) [17]. The chi-squared distribution model with k degrees of freedom distinguishes three different behaviors which can physically describe internal energy levels involved in a ballistic shock/collision: free, kinetic, and elastic twist potential. At start-up of a conducted flow, at sufficiently large Reynolds numbers, in each contact point bursts standing three wave configuration/packets: a faster longitudinal wave on the flow direction and opposite to the velocity of fluid (kinetic energy, E_k) and two transverse waves (free energy E_t, and elastic twist potential E_p). The rapid waves system which represents the reaction of starting impact on the flowing fluid are the lee-wall waves just penetrating the macro-flow field, preserving impact energy in the form of static pressure (potential energy) near equal to the dynamic pressure ($1/2\rho V_\infty^2$, kinetic energy) of flow. The Gaussian distribution curves exhibit two intrinsic properties: affinity of "Ω" – bell shape probability density curves and π – twist of cumulative distribution curves, which can be identified as the intrinsic scales for inertia (rate of inertia e [Kg/s]), and circulation (π [L^2s^{-1}]), respectively, of an impacted fluid. The material integrity/continuity condition requires shocks less g (gravity) which along with their (e, π) scales they can follow two possible routes/scenarios of the inertia: ($2e+\pi$), slow elastic impact preserving its kinetic energy (reversible process) and ($e+2\pi$), fast ballistic impact which is a quasi-ergotic process in the Ehrenfest's sense (irreversible process). But, though the ballistic starting impact, at sufficiently large Reynolds number, have the property of intrinsic stachasticity in the sense that it possess mechanisms of self-randomization, the NSE don't exhibit such mechanisms. *The NSE of which formulation was based on a physical meaningless approximation (*$3\lambda+2\mu=0$*), are misapproachings for describing convoluted contact evolutions, i.e. turbulence.*

The ballistic impact is an entropic shock through which the inertia is halved concomitantly with the inversion of inertia-circulation ratio, preserving its kinetic energy as an oscillatory energy slightly damped [7]. Since the starting shock processes are rapid intrinsic processes, a key outcome is their behavior affined to the macro-flow field for properly selected relativistic parameters and a dimensional exchange between momentum $[1KT^{-1}\times L^2T^{-1}]$ and kinetic energy $[1KL^2T^{-2}]$, so called the "Ω"-shape momentum-kinetic energy invariance for elastic collisions [18].

The relativistic contact effects induced at the beginning of motion are connected to the invariance of mass expressed in the case of fluids by the equation of continuity

$$\frac{d\rho}{dt}+\rho\nabla\mathbf{V}=\frac{D\ln\rho}{Dt}+\nabla\mathbf{V}=0\,, \tag{6}$$

where for an incompressible fluid, with $\rho=\rho_0(\text{const.})$,the equation of continuity assumes the simplified form

$$\theta\equiv\nabla\cdot\mathbf{V}=0\,, \tag{6'}$$

(without starting contact effect).

The zero dilatation (θ) hypothesis is valid only for Mach number $M_\infty<1/3$ i.e. $\frac{\Delta\rho}{\rho_0}<1/2M_\infty^2=0.05$, and this case corresponds to the concept of the perfect (i.e. frictionless and incompressible) fluid, the starting impact of random type halving of impact energy, Fig. 6a (Bernoulli equation). The equation

$$\rho=\rho_0e^{-\theta\delta t},\theta\delta t=2\,, \tag{7}$$

which takes account of the starting contact effect is an early compressibility condition for pre-compressible flows, $1/3\le M_\infty\le 2/3$, i.e. $\frac{\Delta\rho}{\rho_0}<0.15$ (Fig. 7). Equation 7 is the base for the concept of twisted/concentrated boundary vorticity (CBV), introduced some time ago [19], which quantifies the starting compressibility effect through the rate of inertia, e. For a random impact, the rate of inertia $e^\tau,\tau\in\{2,1,0\}$, (τ – integer twist index) follows a slow route, while the ballistic impact produces a fast route with $e^\tau,\tau\in\{2/3,1/2,1/3\}$, ($\tau$ – subunit twist index).

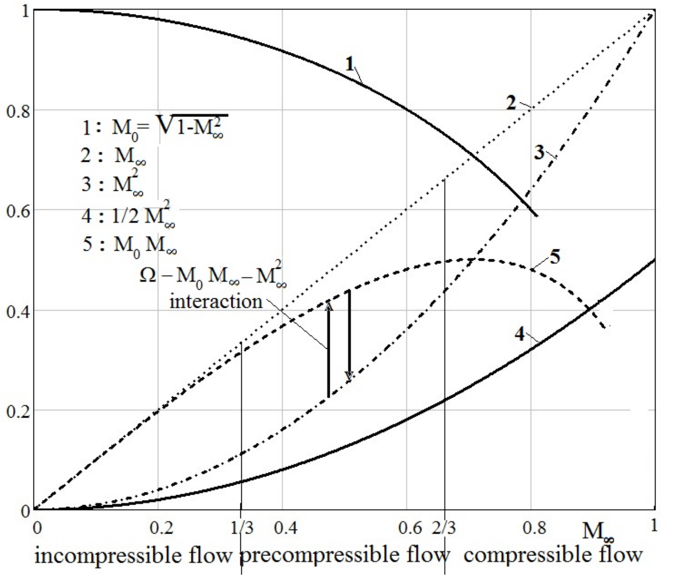

Figure 7 – Definition of pre-compressible (gaseous) flow class including turbulent flow (Mach relativistic effect); the pre-compressibility condition $\log\left(3/2\left(1-M_\infty\right)\right)/M_\infty = 1\pm 0.05$.

The Mach number M_∞ is a **relativistic parameter** (the ratio of speed of undisturbed flow to the speed of sound in the fluid $V_\infty / a_\infty, a_\infty = \left(\gamma p/\rho\right)^{1/2}$) and M_0 is defined as an impact Mach number

$$M_0 \equiv \left(\frac{a_0^2 - V_\infty^2}{a_\infty^2}\right)^{1/2} \approx \sqrt{1-M_\infty^2}$$

which measures the degree of pre-compressibility/pre-stressing occurring during the starting and the product of $(M_\infty \cdot M_0)$ is a starting correction of the momentum, Fig 7. Figure shows firstly that in the range of pre-compressible flows, $M_\infty = 1/3 - 2/3$, the Ω – shape of corrected momentum is coming from the random/momentum starting impact, and secondly, that at $M_\infty = 2/3$, a ballistic/energy starting impact is occurred along with the halving of impact energy (twist potential) and its transfer to kinetic energy by a standing wave system (Fig. 8). The Mach number $M_\infty = 2/3$ (half of the maximum kinetic energy) is the last flow regime affected by starting conditions where the momentum-kinetic energy transfer is occurred by transitional motions associated with self-sustained waves, usually known as turbulent flows.

The threshold of stability for the internal energy is the maximum effective impact pressure that is capable of sliding near zero-shearing friction at the contact interface. This dimensional critical value equal to

$$\mathrm{Re}_{scr} = 1/2\rho_0 a_0^2 = 2/3 \cdot 10^5 \ \mathrm{N/m^2}, \tag{8}$$

(a_0 – sound velocity of air at rest), previously experimentally gained, is defined as a dimensionless static stability parameter/criterion and called Reynolds critical number. Its inverse

$$\mathrm{Re}_{scr}^{-1} \equiv \nu_0 = 1.5 \cdot 10^{-5}\ \mathrm{m^2/s}, \tag{8'}$$

becomes the equilibrium value of kinematic viscosity, that is the minimum effective circulation at near zero-shearing friction. Both theoretical values, based rather on a heuristic reasoning, are consistent with the universal non-linearity Feigenbaum's criterion ($4.669 \approx \log \mathrm{Re}_{scr}$) and viscosity measurements, respectively. The Re_{scr} plays the role of a natural frequency of fluid and ν_0 is the intrinsic scale for internal circulation.

On the other hand, the experimental Reynolds number as a relativistic lump parameter of stability of a flow is the ratio of $(V_\infty l)$, circulation of outer flow (inertial force) to (ν), kinematic viscosity (viscous force), i.e. the internal circulation at the contact surface of molecular nature. The non-recognition of the starting impact as the main flow disturbances has obscured the knowledge and understanding of turbulence phenomenon, values of Reynolds critical number being found only empirically. However, the finding of this parameter which carries information on the overall behavior of the flow field (regardless of much diversity of flow cases) led to the removing of d'Alembert paradox via the Prandtl's boundary-layer theory and the concept of Newtonian viscous fluid.

A more comprehensive interpretation of Reynolds number is connected to the wavy behavior of fluid induced by the twisted flow during the starting as the ratio of wall-bounded to outer flow frequencies

$$\mathrm{Re}_l \equiv \frac{V_\infty l\ \text{(inertia force)}}{\nu\ \text{(viscous force)}} \equiv \frac{V_\infty/\nu\ \text{(frequency of wall-bounded flow)}}{V_\infty/\mathrm{l}\ \text{(frequency of outer flow)}}, \tag{9}$$

where the dimensionless Reynolds number Re_l is a stability standard/control parameter of flow state, so that the flow is statistically stable for $\mathrm{Re} \le \mathrm{Re}_{scr}$ and unstable for $\mathrm{Re} > \mathrm{Re}_{scr}$, playing the role of a current reduced frequency for real fluid motions. The dimensional critical value of Reynolds number Re_{scr} is a switch-limit from the statically stable flow to a dynamically stable flow.

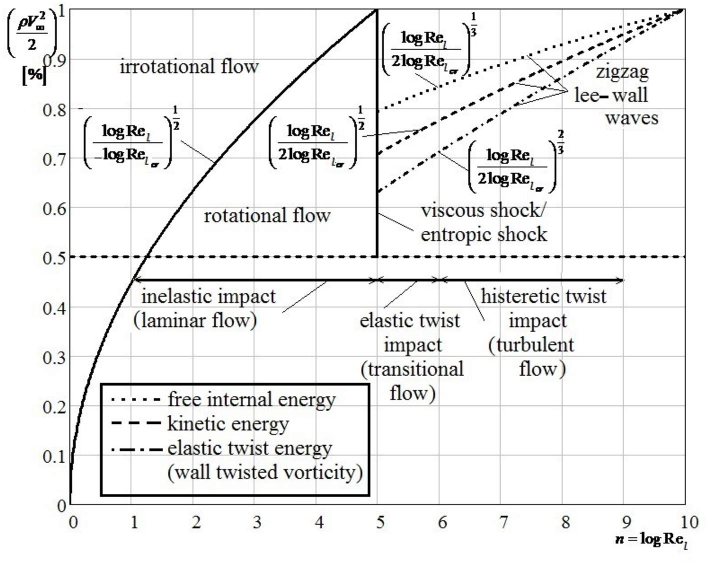

Figure 8 – The ballistic impact/viscous shock associated with standing wall waves (Reynolds relativistic effect)

The current Reynolds number, Eq. 9, is the **second relativistic parameter** of the macro-flow state, which shows the relaxation way of wall-bounded flow after the starting impact.

Figure 8 illustrates the violent relaxation after a ballistic impact so-called weak viscous shock at $\mathrm{Re}_l > \mathrm{Re}_{scr}$, followed by a wall wave system of lee wave type [7]. Figure 9 shows the comparative results of the drag coefficients for flow on a flat smooth plate at zero incidence against the Reynolds number. The present approach based on the impact-twist relationship finds near linear logarithmic dependences for the wave drag coefficients using only a material constant, Re_{scr}.

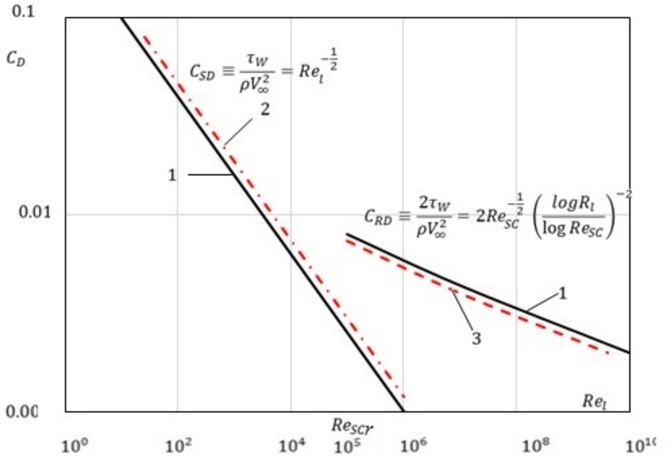

Figure 9 – Drag coefficient/wave drag of flat smooth plates ($\mathrm{Re}_{scr} \approx 10^5$): 1- laminar-turbulent impact theory; 2 – laminar Blasius; 3 – turbulent Schlighting (different authors [2])

Figure 10 illustrates undoubtedly the wave origin of hairpin-vortex packets as lee-wall waves produced by ballistic starting collisions in flows when the Reynolds number exceeds C, where can be considered as a dynamically stable critical value [20], [21]. It is worth to observe that the “hairpin vortex” contact structure is a mechanism of self-sustaining structured turbulence, in principle similar to the intrinsic “flywheel mechanism” in the case of solid bodies. Both mechanisms are the outcome of intrinsic relativistic effects produced by successive elastic collisions between two colliding bodies obeyng Ω – shape momentum-kinetic energy invariance [18]. However, in contrast to the flywheel mechanism which involves a reversible linear/elastic process, the selfsustaining turbulence is an irreversible non-linear/hysteretic en cascade process of the birth-dedh process (BDP) type, Fig. 11, [8], [22].

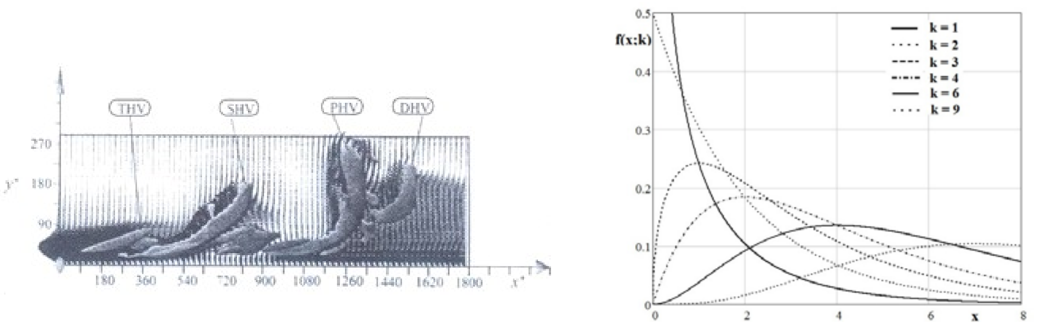

Figure 10 – A comparison between the hairpin-vortex packets and the stochastic model for a ballistic starting impact

The two critical Reynolds numbers divide the pre-compressible flows in friction shearing stable layers ($\mathrm{Re}_{scr} \le \mathrm{Re}_l < \mathrm{Re}_{dcr}$) and rolling friction label layers ($\mathrm{Re}_l \ge \mathrm{Re}_{dcr}$), and the more detailed description of this transition process requests a better concept of the fluid able to permanently adjust itself with the flow state. The dual concept of concentrated/twisted boundary vorticity (CBV) – thixotropic fluid, (already used [7], [8]), is a more realistic concept than the concept of Newtonian viscous fluid (Fig. 11).

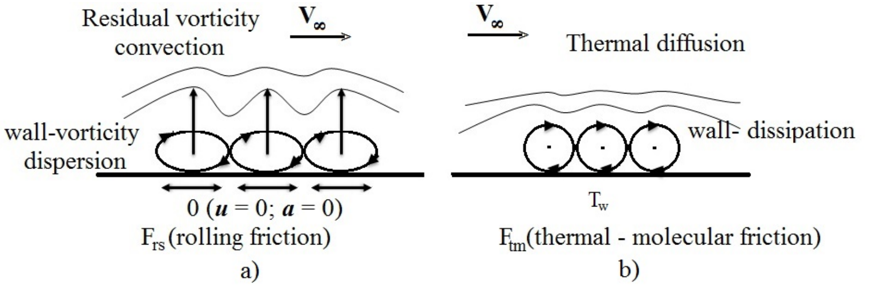

Figure 11 – The Concentrated Boundary Vorticity (CBV) mechanism: a) 2D - Lagrangian structured turbulence (torsion pendulum, $\mathrm{Re}_l \approx 10^7$); b) 3D – Lagrangian structured turbulence (spherical pendulum, $\mathrm{Re}_l \ge 10^8$).

5. CONCLUSIONS

Any turbulent flow involves more or less intermittent motions in two aspects. The first once is the so-called visible, external intermittency associated with the strongly irregular and random movement of macro-flow field or dust-vorticity flow, and the second aspect is the so-called invisible small scale, internal or intrinsic intermittency at the fluid-solid contact surface of molecular nature.

The considerations from this paper are based on a heuristic reasoning and assume the existence of ordered structures, in the sense that the structureless turbulence is meaningless. The claims for structureless turbulence is a reflection of our incapacity to see and understand more intricate aspects of turbulence, that is the convolution, complexity and randomness not synonymous for absence of structure, but rather for its ignorance. The lack of a realistic physical model is the outcome of a century-time misapproching of the turbulence problem. The big misconception of turbulence is the fact that turbulence problem has been thought as a deterministic Cauchy problem, while the complex turbulence phenomenon is a dynamic stochastic phenomenon associated with relativistic effects of molecular nature.

The present paper comes to remove this historical drawback by introducing the concept of twisted/concentrated boundary vorticity (CBV) via the topology of twisted contact structures based on contact geometry, and by thinking the physical prototype of turbulence as a collision-like process of momentum-kinetic energy exchange between flowing fluid and its impacted solid boundary, within a short time of contact, at the onset of motion. The process called starting impact/shock occurs in the case of flows for the Mach number range of $M_\infty = \left(1/3 - 2/3\right)$, where the wall pre-compressibility effects or wall torsion pressures are responsible for the wavy behavior of all wall-bounded gaseous flows, called so forth precompressible flows. The starting-collision process associated with wall waves is a universal process for all precompressible flows obeying a "Ω"-shape momentum-kinetic energy invariance easily observed in the case of turbulent jet-like flows (see their bell shaped similar profiles). Two intrinsic scales of inertia (e) and circulation (π) have used in the stochastic models of starting impact for describing the macro-flow field of the canonical Prandtl boundary-layer flow where the wall torsion pressure and the frictional wave drag are more realistic models than Lighthill's BVF mechanism and Prandtl's wall law. The details of the wall-zigzag wave system produced in the vicinity of solid walls are found in our previous paper [7], [8]. The wall-zigzag waves are a permanently presence around the all wall-bounded flows regardless of their flow state, laminar or turbulent, for the Reynolds number range of $\mathrm{Re}_{l,ind} = 10^{\pi}$ (the low indifference Reynolds number, Tollmien-Schlighting waves) up to $\mathrm{Re}_{h,ind} = 10^{3\pi}$ (the high indifference Reynolds number, i.e. the end of turbulence process where the equilibrium thermodynamic state of $\frac{p}{\rho^{e^{1/3}}} = \frac{p}{\rho^{\gamma}} = const.$ is reached).

The main outcome of the present study is the definition of precompressible flows as a distinct class by the pre-compressibility condition $\log\left(3/2\left(1-M_{\infty}\right)\right)/M_{\infty} = 1 \pm 0.05$, which includes all turbulent shear gaseous flows obeying "Ω"-shape momentum-kinetic energy invariance. Besides the elucidating of some controversial basic issues of turbulence as large Re ($\mathrm{Re} = 10^{2\pi} - 10^{3\pi}$, [7], [8]), zero viscosity limit $\left(\nu = \nu_0^{1+2/3} \approx 10^{-8} m^2/s\right)$ and relevance of the Euler equations (Beltrami flows displaying the phenomenon of Lagrangian turbulence [23]), the paper is important from the standpoint of continuum mechanics by filling the gap, reflected by the NSE, between the scales of molecular motions and the smallest relevant scales in fluid flows including turbulence. The results found in the present investigation, largely based on physical considerations, are consistent with the Robert & Sommeria's equilibrium statistical-mechanical theory for the continuum 2D Euler equations [24].

REFERENCES

[1] J. R. d'Alembert, *Paradoxe proposé aux géomètres sur le résistance des fluids*, in Opuscules mathématiques, vol. **5** (Paris), Mémoire XXXIV, #I, pp. 132-138, 1768.

[2] H. Schlichting, *Boundary Layer Theory*, McGraw-Hill Book Company, New York, 1968.

[3] P. Constantin, *Some open problems and research directions in the mathematical study of fluid dynamics*, Springer Verlag, Berlin, pp. 353-360, 2001.

[4] C. Fefferman, *Existence and smoothness of the Navier-Stokes equations*, http://claymath.org/ (Millenium-Prize-Problems/ Navier-Stokes-Equations, Clay Mathematics Institute, 2000.

[5] C. Foias, What do the Navier-Stokes equations tell us about turbulence, *Contemporary Mathematics*, **208**, pp, 151-180, 1997.

[6] O. A. Ladyzhenskaya, Mathematical analysis of NSE for incompressible liquids, *Annual Rev. Fluid Mechanics*, **7**, pp. 249-272, 1975.

[7] H. Dumitrescu, V. Cardos, R. Bogateanu, The transition process for laminar to turbulent flows, *ECCM-ECFD 2018, Glasgow*, June 11-15, 2018.

[8] H. Dumitrescu, V. Cardos, The origin of shear turbulence, *INCAS BULLETIN*, vol. **9**, issue 4, (online) ISSN 2247–4528, (print) ISSN 2066–8201, ISSN–L 2066–8201, DOI: 10.13111/2066-8201.2017.9.4.7, pp. 75-89, 2017.

[9] S. Lie, *Geometrie der Berührungstransformation*, Teubner, Leipzig, 1896.

[10] H. Geiger, A brief history of contact geometry and topology, *Expositions Mathematicae*, **19**, pp. 25-53, 2001.

[11] R. Lutz, Sur la géomètrie des structures de contact invariantes, *Ann. Inst. Fourier, Grenoble*, **29**, no. 1, pp. 283-306, 1979.

[12] J. W. Gibbs, Graphical methods in the thermodynamics of fluids, *Trans. Connecticut Acad. Arts Sci.*, **2**, pp. 309-342, (1871-73).

[13] F. Verheest, *Waves in Dusty Space Plasma*, Kluwer Academic Publishers, Dordrecht, 2001.

[14] C. B. Lee, Possible universal transitional scenario in a flat plate boundary layer: measurement and visualization, *Physical Review E*, **62**, 3, pp 3659-3670, 2000.
[15] A. Tsinober, *The essence of turbulence as a physical phenomenon*, Springer Dordrecht, Heidelberg, New York, London, 2014.
[16] C. L. Olson, M. G. Olsson, Dynamical symmetry breaking and chaos in Duffing's equation, *Am. J. Phys*., **59**, pp. 907-911, 1991.
[17] H. O. Lancaster, *The Chi-squared Distribution*, J. Wiley, 1969.
[18] O. Onicescu, *Mecanica (Mechanics)*, Technical Publishing House, Bucharest, 1969.
[19] H. Dumitrescu, V. Cardos, I. Malael, Boundary vorticity dynamics at very large Reynolds number, *INCAS BULLETIN*, vol. **7**, Issue 3, (online) ISSN 2247–4528, (print) ISSN 2066–8201, ISSN–L 2066–8201, DOI: 10.13111/2066-8201.2015.7.3.8, pp. 89-100, 2015.
[20] J. Zhou, R. J. Adrian, S. Balachander, T. M. Kendall, Mechanisms for generating coherent packets of hairpin vortices in channel flow, *Journal of Fluid Mechanics*, vol. **387**, pp. 353-396, 1999.
[21] R. J. Adrian, Hairpin vortex organization in wall turbulence, *Physics of Fluids*, **19**, 041301, pp. 1-16, 2007.
[22] P. R. Parthasarathy and R. B Lenin, Birth and Death Process (BDP) Models with Applications, *American Series in Mathematical and Management Sciences*, **51**, Syracuse, NY, American Sciences Press, Inc. 2004.
[23] J. Etnyre, R. Ghrest, *Contact topology and hydrodynamics*, University of Texas, Austin, TX78712, pp. 1-15, 1997.
[24] R. Robert, J. Sommena, Statistical equilibrium states for two-dimensional flows, *Journal of Fluid Mechanics*, vol. **229**, pp. 291-210, 1991.